ISSN 1573-160X, *PHYSICAL OCEANOGRAPHY*, Vol. 30, Iss. 4, pp. 410-427 (2023)

published in *Morskoy Gidrofizicheskiy Zhurnal*, 2023, Vol. 39, Iss. 4, pp. 448-466.

Original article

Trends and Regional Features of Variability of the Northeast Pacific Ocean Thermal Conditions North of 30°N over the Last Four Decades

I. D. Rostov ✉, E. V. Dmitrieva, N. I. Rudykh

V. I. Il'ichev Pacific Oceanological Institute, Far Eastern Branch of Russian Academy of Sciences, Vladivostok, Russian Federation
✉ *rostov@poi.dvo.ru*

Abstract
Purpose. The study is purposed at revealing the regional features of modern climatic changes in water temperature in the northeastern extratropical zone of the Pacific Ocean, at assessing the characteristics of temperature trends on the ocean surface and in its upper layer and their relationship with the large-scale processes in the ocean and atmosphere.
Methods and Results. Based on the NOAA climatic data sets, and using the statistical methods of analysis and the apparatus of empirical orthogonal functions, the characteristics of the interannual variability of water temperature on the surface and in the upper 1000-meter layer were determined in different regions of the area under study. Temperature trends, correlations with the influencing factors and their statistical significance for some 20-year periods of previous 40 years were quantitatively assessed.
Conclusions. In the first decades of the 21st century, the warming trends are explicit on the surface and in the upper 200-meter layer of the northeastern and central regions of the area. As compared to the previous 20-year period, the magnitude of positive SST trends increased, on average, by about 4 times over the entire water area. In course of the past two decades, the heat content of the upper 200-meter layer increased by 5% and that of the whole 1000-meter layer – by 2%, which is 1.5 times less than in the northwestern sector of the Pacific extratropical zone where, unlike the surface, the rate of water column warming was higher. As for the area under study, on the whole, the correlations between the heat content fluctuations in the upper 200-meter ocean layer and the changes in influencing factors are manifested through the climatic indices *NPGO*, *PDO*, *NP*, *PNA*, *SOI*, *AD* and the atmospheric pressure gradients between the leading centers of the atmosphere action.

Keywords: northeastern part of the Pacific Ocean, extratropical zone, modern climate changes, regional features, water temperature, heat content, warming trends, climate indices, correlations

Acknowledgments: The work was carried out within the framework of the state assignment of POI FEB RAS on theme 0211-2021-0008. State registration No. 121021700346-7. The authors are thankful to the program developers for the possibility to use the climatic data posted on the NOAA sites. The authors are grateful to the reviewer for constructive comments.

For citation: Rostov, I.D., Dmitrieva, E.V. and Rudykh, N.I., 2023. Trends and Regional Features of Variability of the Northeast Pacific Ocean Thermal Conditions North of 30°N over the Last Four Decades. *Physical Oceanography*, 30(4), pp. 410-427.

Introduction

The study area of the Pacific Ocean is bounded in the north by the arc of the Aleutian Islands, in the eastern and northeastern parts – by the North America coast, in the west – by the 180° meridian, and in the south – by 30°N. Its northern part is located in the area of distribution of the transformed subarctic water structure, the southern part is subtropical, and the central part belongs to the transitional

region, where between 40–45°N there is a zone of the subarctic (northern polar) front, which extends to 57°N in the Gulf of Alaska [1] and gradually erodes from the west to the east. In this band, a transition from warm and saline subtropical waters to cold, fresher subarctic waters [2] takes place, and the Subarctic and North Pacific currents directed to the east are traced [3–5]. As they move towards the coast of North America, their general flow bifurcates. The northern branch forms the cyclonic Alaska Gyre, which includes the Alaska Current, which moves northwest off the coast of Alaska and further southwest along the Aleutian Islands. The other branch deviates to the southeast, forming the flow of the coastal California Current in the system of the subtropical gyre [3]. Under the effect of strong stratification, seasonal changes in water temperature (T_w) at different levels in this area are observed mainly in the upper layer of 100–250 m. At a depth of 100 m, the phase of the seasonal cycle of temperature fluctuations lags behind the phase at the surface by two to three months [6, 7]. As noted earlier [8], the weather and climate conditions in this area depend on the interaction of three main baric formations that are seasonal atmospheric centers of action (ACA): the Aleutian Low, the North Pacific (Hawaiian) High, and the Siberian winter anticyclone, which determine the characteristics of heat exchange between the ocean and the atmosphere, pressure fields, wind and the state of the upper ocean layer. Global warming affects pressure distribution in the atmosphere and in individual ACAs, as well as strength and location of jet streams above the polar frontal zone, an area of sharp thermal contrast between cold polar and warm tropical air. The characteristics of ACA and jet streams are driving factors of weather in mid-latitudes [9].

In the study area, there is a habitat and feeding area for various species of Pacific salmon, which spawn in the rivers of the Subarctic Pacific Ocean coastal zone and are the most important object of fishing. Modern climatic changes occurring in various geospheres can cause a devastating impact on marine ecosystems and negative economic consequences. Thus, since 2013, after the end of the pause in global warming [10, 11], the so-called marine heat waves, local areas with extremely high ocean surface temperatures related to atmospheric effects [12–15], have become a common and widespread phenomenon in the northeastern part of the Pacific Ocean [12–15]. In 2014–2016 and 2019–2020, these areas with SST anomalies up to 2.5–3°C propagated along the western coast of North America and to the most of the northeast Pacific Ocean, forming three-dimensional thermal structures covering the upper layer of the ocean several hundred meters thick and persisting for a long time [12]. During these events, the phase of T_w variations at 200–300 m levels lagged behind the SST changes by several months [14, 15]. These phenomena have had an unprecedented biological impact on the numerous trophic levels of marine ecosystem, the number of different zooplankton taxa and, as a result, on the biomass of fish stocks [15, 16].

The relationships between the intensity, duration, and scale of this phenomenon with the characteristics of the atmospheric pressure field, wind, and the phases of such large-scale atmospheric-ocean interaction processes as the El Niño – the Southern Oscillation (ENSO), decadal (*PDO*), and interdecadal (*IPO*) Pacific Ocean Oscillations are complex and ambiguous, as they have many overlapping spatial and temporal scales [17] and are the subject of ongoing research. They note that the past 6–7 years have become the warmest in the history of observations in

the study area. By this time, a pause in global warming was over, after 2016 the Aleutian Low weakened, and the intensity index of the large-scale North Pacific Gyre Oscillation (*NPGO*), which reflects the trends in oscillations in the wind regime, ocean level, and SST, passed into a negative phase.

In general, in the region of the Subarctic Pacific Ocean, the warming patterns over the past 4 decades are expressed in the trends of interannual variability of air temperature and SST (on average ~ 0.20 °C/10 years) with significant regional differences (by 1.5–2 times) of the ongoing changes [8, 18]. At the same time, in the west of the region, the warming rate is higher than in the east, where temperature trends over the specified period were minimal or statistically insignificant. At the same time, under effect of shifts in the climate regime observed in recent decades, separate phases with different warming rates are distinguished [19], therefore, estimates of temperature trends for these periods, as well as interpretation of their causes, are sensitive to the calculation period and may differ from estimates for long-term period [20, 21]. Thus, in the 1998–2013 interval the rate of the global mean surface temperature increase slowed down compared to the second half of the 20th century, which was the subject of targeted research [14]. The characteristics of the vertical structure of water temperature and heat content trends, which are not well understood due to the relatively small number of oceanographic observations in this area, are closely related to this phenomenon. In recent years, promising systems (models) for the assimilation of oceanographic data, such as SODA and GODAS [22], have been increasingly used in ocean climate research. So, over the 2000–2021 period in the study area, the share of information entering the databases [23] and the GODAS system from the observation network of ARGO profiling floats increased to 127.1 thousand profiles (excluding the Bering Sea). Further, in this work, we used the GODAS data on T_w exactly for the last 20-year period.

The purpose of the research is to reveal the regional features of modern climatic changes in water temperature in the northeastern part of the extratropical zone of the Pacific Ocean over separate 20-year periods, to determine the quantitative characteristics of temperature trends at the surface and in the upper layer of the ocean, and to assess their relationship with large-scale processes in the ocean and the atmosphere.

This paper is a continuation of the research by the authors on the features of the interannual variability of the water and air thermal characteristics in the waters of the Subarctic Pacific Ocean and the northwestern part of the extratropical zone of the Pacific Ocean, which are observed under the conditions of modern global warming [8, 18, 24].

Data and methods

The following data from NOAA climate arrays were used:

– ocean surface temperature for 1982–2021 (https://psl.noaa.gov/data/gridded/data.noaa.oisst.v2.html);

– T_w at different levels of the GODAS oceanographic data assimilation system [22] (https://www.esrl.noaa.gov/psd/data/gridded/data.godas.html) for 2000–2021;

– reanalysis data of pressure fields, wind and heat fluxes on the ocean surface and series of climate indices (CI) [24] (https://psl.noaa.gov/data/gridded/index.html, https://psl.noaa.gov/data/climateindices/list/).

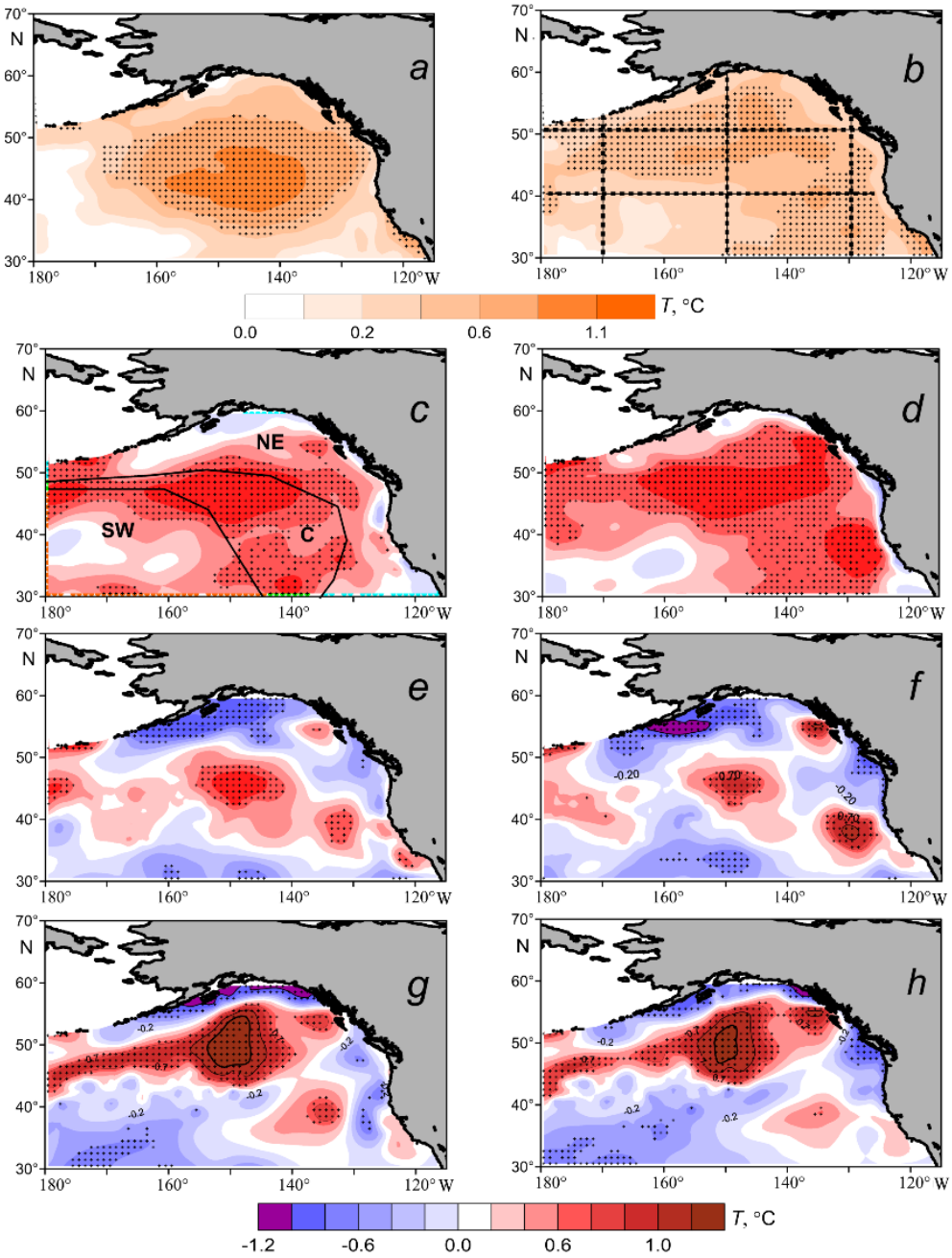

F i g. 1. Values of the SST trend (°C/10 years) (*a*, *b*) and the normalized heat content anomalies ΔQ_T, (non-dimensional units/10 years) in the layers 5–200 m (*c*, *d*), 200–460 m (*e*, *f*) and 460–950 m (*g*, *h*) in the warm (*left*) and cold (*right*) seasons in 2002–2021. Here and below, crosses denote the grid nodes where the estimates are 95% statistically significant [8]. Fragment *b* shows the locations of sections, and fragment *c* – the selected warm-season areas (NE, C and SW)

Additionally, the index of the difference in atmospheric pressure at sea level between the ACA (atmospheric centers of action) – the Hawaiian High and the Aleutian Low (*H-NP*) was calculated. Statistical analysis and decomposition of

the anomaly fields of the studied series into principal components of empirical orthogonal functions (EOFs) were carried out according to a unified method [8, 24] for warm, summer (June – September) and cold, winter (November – March) seasons (periods) of the year. Also, the values of the integral temperature anomalies (ΔQ_T) – an indicator of heat content [25] at the grid nodes of 0.3° × 1° for different layers from near-surface to 1000 m were calculated. According to the data on the ΔQ_T interannual variability in the 5–200 m layer, using the EOF methods and cluster analysis, three regions were identified within the study area: northeastern (NE), central (C), and southeastern (SE) (Fig. 1, *c*). As a result of grid data averaging within these areas, series of interannual fluctuations of T_w anomalies at different levels and integral temperature in separate layers were formed: upper (5–200 m), intermediate (200–460 m), and deep (460–950 m).

Features of spatial and interannual variability of water temperature

The system of waters of the Alaska Gyre, as well as the cold Alaska and California currents, is located within the boundaries of the northeastern region. In the sector of the central region, a transitional area (or water mixing area) of two structural zones is distinguished, and in the southwestern region, predominantly subtropical waters are distributed [3, 5] (Fig. 1, *c*).

When comparing Fig. 1, *a*, *b* and 2, it can be seen that, despite the slowdown in the SST growth rate and the pause in global warming since the late 1990s, the current 20-year period of the beginning of the 21st century was characterized by a higher warming rate than at the end of the 20th century. This is confirmed by the corresponding quantitative estimates given in Table 1.

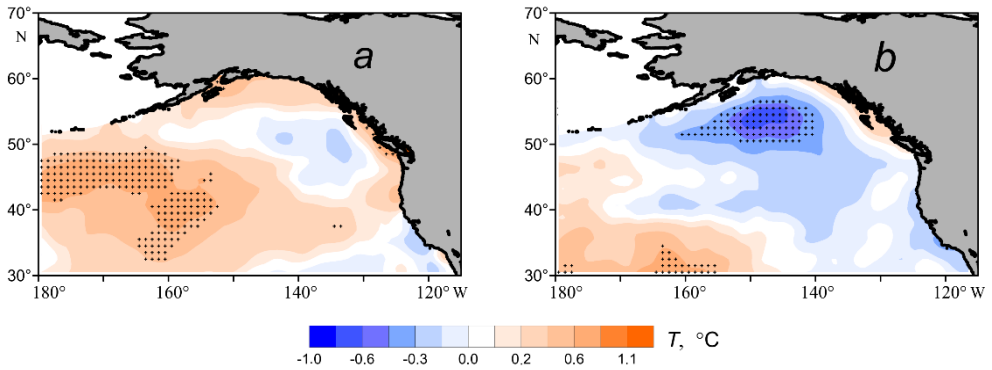

F i g. 2. Values of the SST trends (°C/10 years) in warm (*a*) and cold (*b*) seasons in 1982–2001

In the first decades of the 21st century, warming trends in the upper 1000 m layer both in the warm and cold seasons are expressed the best at the surface and in the upper 200 m layer of the northeastern and central regions (Fig. 1, a – *d*). In some years of this period (2014–2016 and 2019–2020), extreme anomalies in the average annual SST values were observed (on average for the regions ~ 1.3 ºC). In comparison with these years, in the previous 20-year period (1982–2001), the trends in the interannual SST variation were significantly weakened (Fig. 2).

Table 1

Trends in interannual changes of the SST anomalies in the identified domains for two periods: 1982–2001 and 2002–2021

Area	σ^2	*b*	*D*	*tr*	b_w	b_c
1982–2001						
NE	0.12	0.02	0	0.0	0.13	-0.13
C	0.20	0.02	0	0.0	0.24	-0.11
SW	0.20	0.30	16	0.6	**0.47**	0.23
Whole area	0.06	0.10	5	0.2	**0.28**	0.00
2002–2021						
NE	0.37	0.41	20	0.8	0.41	**0.48**
C	0.35	**0.56**	39	1.1	**0.73**	**0.53**
SW	0.18	**0.34**	15	0.7	**0.35**	0.30
Whole area	0.17	**0.44**	40	0.9	**0.49**	**0.44**

N o t e. σ^2 is the variance of the average annual SST; *b* is the slope coefficient of the average annual temperature linear trend (°C/10 years); *D* is the trend contribution to the total variance (%); *tr* is the trend over the observation period (°C); b_w, b_c are the values of *b* for the warm and cold seasons. Here and in the other tables, statistically significant (95%) estimates are highlighted in bold.

During the cold season of 1982–2001 period, an anomalous cooling was observed at the ocean surface in the NE and C regions (Table 1, Fig. 2, *b*) in the area of the cyclonic Alaska Gyre, which occurred simultaneously with its intensification [4]. During the second period, against the background of an increase in the variance of fluctuations in the SST anomalies (SSTA), the value of positive trends on average over the entire water area increased by about 4 times, i.e. the SST increase significantly accelerated (Table 1). This is the difference between the water area under consideration and the region of the northwestern part of the Pacific Ocean extratropical zone [24], where the opposite trend was observed. As it was demonstrated earlier [18], the interannual fluctuations of SSTA in these areas are in antiphase. A preliminary analysis of the interannual variability of baric topography field characteristics revealed that one of the possible causes for the difference in the warming rate in these areas are changes in the position and intensity of the Aleutian Low [24, 26].

In the underlying intermediate and deep layers in different domains of the study region, extensive areas of statistically significant trends of the integral temperature anomalies (ΔQ_T) are observed with a maximum positive value up to 1.2 non-dimensional units/10 years in the Alaska Gyre region and negative values up to –1.2 non-dimensional units/10 years in the intermediate and deep layers along the edges of the coastal shelf (Fig. 1, *e* – *h*). Here, in the areas of the North American continent coastal zones, a variation in the wind regime characteristics causes coastal upwelling of colder deep waters to the surface, which has a significant effect on the heat content of waters and the state of marine ecosystems [3, 27]. Another area of significant negative trends in ΔQ_T is traced in the north of the NE region in

the Alaska Current water system, and the third one is in the SW region. It should be noted that the total area and volume of the intermediate and deep layers, where the warming of the study area water column is observed, is much smaller than in the area of the northwestern part of the ocean [24], where this process proceeds at a higher rate.

The main features of the spatial structure of integral temperature interannual fluctuations in the upper layer of 5–200 m over the past 20 years are characterized by the following specifics. The first three modes of the EOF expansion of ΔQ_T field both in the warm and cold seasons describe ~ 70% of its total variance. The first, most energy-carrying mode (37% of the dispersion) reflects the main feature, i.e. antiphase fluctuations of the integral temperature in the NE – C and SW regions, while the second and third (33% of the dispersion) reflect smaller features of the trend field ΔQ_T in the 5–200 m layer (Fig. 1, *c*; 3).

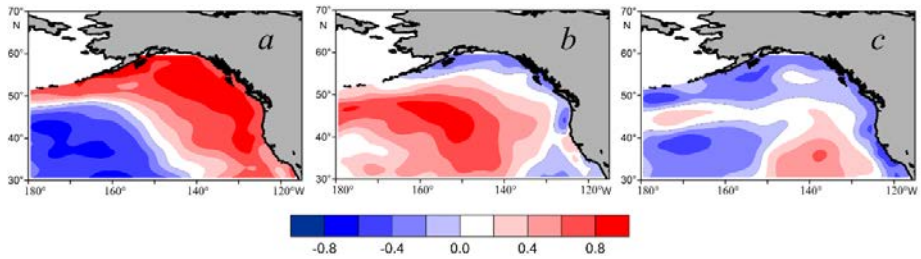

F i g. 3. Spatial distribution of the coefficients of the first (*a*), second (*b*) and third (*c*) EOF modes of the integral temperature anomalies ΔQ_T (non-dimensional units) in the 5–200 m layer for the warm season in 2002–2021

Subsequently, the obtained results of the fluctuation field ΔQ_T decomposition into components were applied to identify correlations between the variability of the thermal conditions of the water area under study and the characteristics of large-scale processes in the ocean and atmosphere.

Interannual variability of upper 1000-meter layer thermal characteristics

A visual representation of the features of T_w vertical distribution interannual variability, the range of its oscillations and the trend at different levels in the central regions of the identified areas is given in Fig. 4. The seasonal cycle can be traced mainly in the upper 100 m, which was also noted before the onset of the modern warming phase [6]. The maximum values of T_w fluctuations (> 2 °C) were observed in the upper 50–100 m layer of all regions (in the SW region – in the cold season down to 150 m depth) (Fig. 4, *b*, *e*, *h*), and the relation between the temperature variations at different levels is manifested in the vertical profiles of the T_w anomaly trends (Fig. 4, *c*, *f*, *i*). In all areas, in different parts of the upper 300–350 m layer, warming is observed in both seasons. In the underlying layers of 200–400 m thickness, the sign of the temperature trend changes to the opposite one, and deeper than 600–800 m it again becomes positive. As noted earlier [14, 15], the phase of T_w changes at the 200–300 m horizons lags behind the SST changes by several months or more. At the same time, due to the limited length of the series and the nature of

the amplitude-frequency composition of oscillations, statistically significant trends in T_w are distinguished only within the upper 200–300-m layer and in individual layers of the water column lower sections.

Over the past 20 years, in the water column of the upper 5–200 m layer in the identified areas, the average integral temperature (as well as heat content) increased by 4–8%, and in the entire 1000 m layer by 2%, which is 1.5 times less than in the northwestern sector of the Pacific Ocean extratropical zone [24].

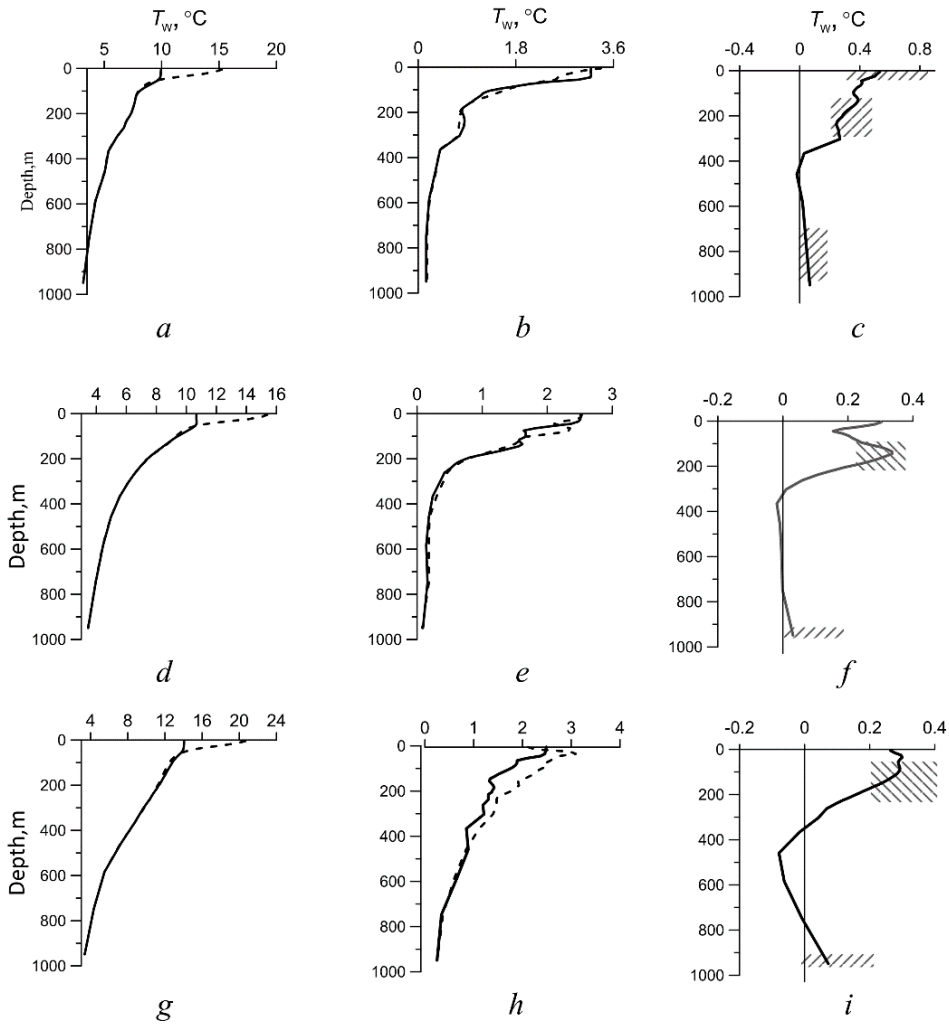

F i g. 4. Generalized curves of vertical distribution T_w (*a, d, g*), range of its changes (*b, e, h*) in the warm (dotted line) and cold (solid line) seasons, and trend of the average annual T_w (*c, f, i*) in 2000–2021. From top to bottom: the NE, C and SW areas. Hatching marks the layers with the 95% statistically significant values in the average annual water temperature trends

Comparison of Fig. 1, *c* – *h*; 4 and 5 enables us to consider the features of a three-dimensional structure of warming (cooling) temperature trends on zonal and meridional sections in the study area. In all sections, the largest statistically

significant positive trends are observed in the upper 200–300 m layer, while negative trends are observed mainly within the intermediate layer (Fig. 5).

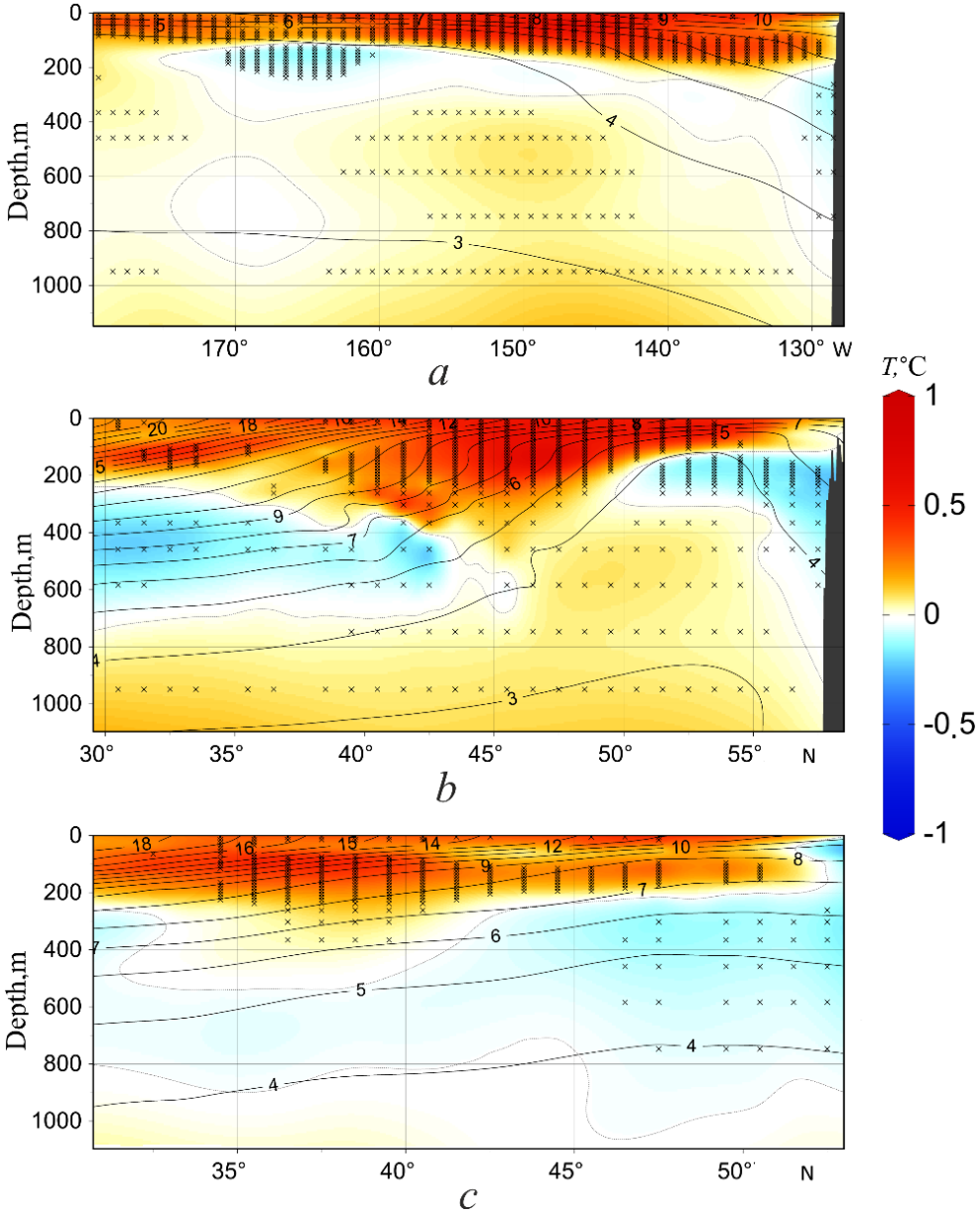

F i g. 5. Joint vertical distribution of the average annual T_w (contrasting lines) and the trends in temperature anomalies (ºC/10 years) (highlighted in color) for 2000–2021 on the zonal section along 50° N (*a*) and the meridional sections along 150° W (*b*) and 130° W (*c*). Section locations are shown in Fig. 1, *b*

The zonal section along 50°N is located near the boundary of the NE and C regions on the southern periphery of the cyclonic Alaska Gyre. In the west, it crosses

one of the branches of the Alaska Current [5], which may be associated with an area of significant negative trends in T_w at 100–200 m depth between 160° and 170°W. In the eastern part of the section, negative trends are traced in the upwelling zone [27] (Fig. 5, *a*), and the area with the largest significant positive trends in T_w (~ 1 °C/10 years) throughout this entire section, as in the other zonal section at 30°N (other zonal sections are not demonstrated), is located in the upper 100–200 m layer. At the third section along 40°N, located in the subarctic front zone [1, 3], the lower boundary of this layer deepens to 300–400 m. At meridional sections along 170°, 150° and 130°W, the warming trends are also well-manifested in the upper layer of the subarctic (polar) front (Fig. 5, *b*, *c*), and cooling trends – in the intermediate layer in the southwest and north of the water area, which is in good agreement with the integral temperature trend maps (Fig. 1, *e*, *f*).

Correlations of thermal characteristic variability with large-scale and regional processes in the ocean and atmosphere

A cross-correlation and regression analysis of interannual variations in the time series of SST anomalies with variations of climate indices and other parameters characterizing the state and dynamics of the climate system was carried out over two periods: 1982–2001 (period I) and 2002–2021 (period II), as well as ΔQ_T anomalies in separate layers for the second period. As noted earlier [8], one of the indicators characterizing the baric system state is a geopotential field of isobaric surface AT_{500} (hPa) in the middle troposphere, and variations in geopotential anomalies (ΔH_{500}) in the region are closely related to fluctuations in SST, wind field, and various climatic indices. During 1982–2021, in most of the study area in both seasons, during the transition from the first to the second period, a change in the sign of the trend of ΔH_{500} anomalies and a deepening of the area of its positive values near the Aleutian Low were observed [24]. At the same time, due to the restructuring of the atmospheric circulation, the magnitude and sign of the trends in climate indices (*b*), as well as the nature of the correlations between SST fluctuations and the most significant CIs, also changed (Table 2).

In the region overall, due to the atmosphere circulation variations, the signs of correlations between the variations in SST, leading modes of geopotential anomalies ΔH_{500} and *PDO* for both 20-year periods during the warm season changed to the opposite ones. At the same time, the remote effect of the Asian Depression (AD) and the dependence of SST variations on the trends in level surface fluctuations and ocean circulation characteristics (*NPGO*) increased, and in the winter season, the correlations with fluctuations of *H-NP* (an indicator of the atmospheric pressure gradient between the two leading ACAs) weakened. In addition, in the selected areas, noticeable and statistically significant correlation coefficients of SST fluctuations with other indices – *IPO* and *EP-NP*, the values of which are not given in Table 2, took place. At the same time, although the characteristics of the Aleutian Low (*NP*) are here one of the main indicators of the climate system state [28],

the changes in *NP*, *IPO*, *PDO*, and *NPGO* are interrelated and occur quasi-synchronously through atmospheric connections.

Table 2

SST correlation coefficients for the selected regions of the northeastern Pacific Ocean with climate indices in the warm and cold (in brackets) seasons for two periods during 1982–2021

Index	$K_1\Delta H_{500}$	*PDO*	*NP*	*NPGO*	*H-NP*	*PNA*	*AD*
1982–2001							
NE	-0.4 (**-0.5**)	**0.5** (**0.8**)	- (**-0.5**)	0.4 (-0.3)	- (0.3)	-0.4 (**-0.6**)	0.3 (-)
C	-0.4 (0.4)	-0.2 (0.0)	- (0.2)	-0.3 (**-0.6**)	- (**-0.6**)	-0.3 (0.4)	0.1 (-)
SW	0.1 (**0.7**)	**-0.8 (-0.9**)	- (**0.6**)	0.4 (0.0)	- (**-0.5**)	-0.3 (**-0.5**)	**-0.5** (-)
Whole area	-0.3 (**0.5**)	-0.2 (-0.2)	- (0.3)	-0.1 (**-0.6**)	**- (-0.7**)	-0.2 (**-0.6**)	0.0 (-)
2002–2021							
NE	0.0 (0.0)	**0.8** (**0.8**)	- (-0.4)	**-0.8** (**-0.5**)	**- (**0.0)	0.1 (0.3)	**0.5** (-)
C	**0.7** (0.2)	0.4 **(**0.2)	- (0.1)	**-0.7 (-0.6**)	- (-0.3)	0.1 (-0.1)	0.4 (-)
SW	0.0 (**0.5**)	**-0.6** (**-0.8**)	- (**0.8**)	-0.1 (-0.3)	- (**-0.5**)	0.0 **(-0.7**)	**-0.5** (-)
Whole area	**0.6** (0.3)	0.4 (0.2)	- (0.2)	**-0.7 (-0.8**)	- (-0.4)	0.1 (-0.2)	0.3 (-)

Note: $K_1\Delta H_{500}$ are the EOF time coefficients of the first mode of the geopotential anomaly variations.

In the last two decades, the corresponding correlations of integral temperature variations in the 5–200 m layer and various indices manifest themselves most extensively (in terms of the area of effect, duration, and correlation coefficient) with the following CIs: $K_{1\text{-}2}\Delta H_{500}$, *NPGO*, *PDO*, *NP*, *PNA*, *SOI*, *AD*, as well as with *H-NP*. Some pairwise regression maps of these relationships are shown in Fig. 6.

The main features of the spatial distribution of the studied characteristics are in good agreement with each other, since the regimes of climatic variability in the study area, parameterized by various CIs associated with atmospheric effects [12], are not independent. The bimodal structure of the field of the considered regression relationships is well-expressed on all maps, which is consistent with the distribution of trends in the temperature anomalies (Fig. 1, *c*, *d*), SST (Fig. 2), and leading modes of EOF ΔQ_T (Fig. 3).

The first three EOF modes of interannual fluctuations in the field of the integral temperature anomalies of the upper 5–200 m layer (ΔQ_T), which describe the main features of its structure and 70% of variability, are closely related to large-scale processes in the ocean and atmosphere through the corresponding climatic indices (Table 3). At the same time, statistically significant relationships of the third mode $K_3\Delta Q_T$ with the considered CIs are not expressed.

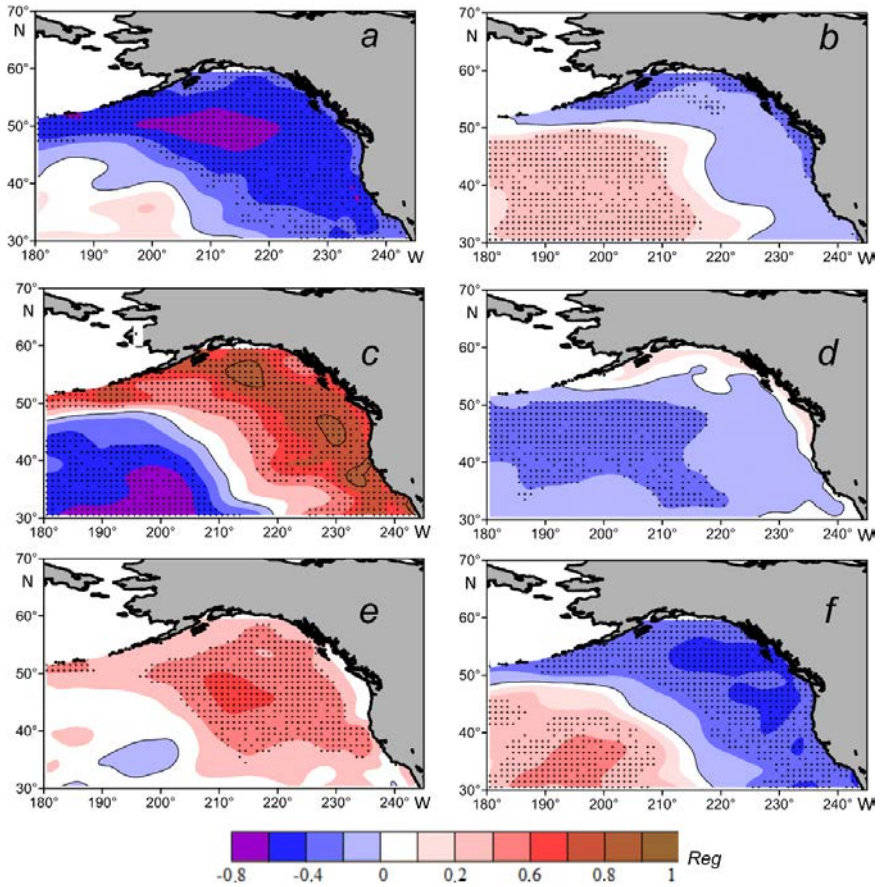

F i g. 6. Linear regression coefficients (*Reg*) of fluctuations in the anomalies of average annual values of the integral temperature (ΔQ_T) in the 5–200 m layer with the climatic indices *NPGO* (*a*), *PDO* (*c*) and $K_1\Delta H_{500}$ (*e*) in the warm (*left*), and *NP (b)*, *H-NP (d)* and *SOI (f)* in the cold (*right*) seasons in 2002–2021

T a b l e 3

Correlation coefficients of the average annual values of the EOF anomaly principal components of the average annual integral temperature in the 5–200 m layer with different CIs in 2002–2021

Parameter	*PDO*	*NP*	*NPGO*	*H-NP*	*PNA*	*AD*	*SOI*	$K_1\Delta H_{500}$	$K_2\Delta H_{500}$
$K_1\Delta Q_T$	**0.8/0.8**	-/-0.2	**-0.7/-0.7**	-/-0.1	0.0/0.2	**0.6**/-	-0.3/**-0.6**	0.4/0.0	**-0.5**/**-0.6**
$K_2\Delta Q_T$	0.2/-0.4	-/**0.5**	**-0.6**/-0.4	-/**-0.5**	0.4/-0.5	-0.1/-	0.2/-0.1	**0.5/0.5**	0.0/0.2

N o t e. K_1, K_2 are the EOF time coefficients of the first modes of decomposition of the ΔQ_T and ΔH_{500} fields.

For most climatic variables, the density of statistically significant correlations of ΔQ_T interannual fluctuations in the upper layer with different CIs weakens with

increasing depth, mode number, and its contribution to the total dispersion of integral temperature variability. Temperature variations occur not only at the surface, they propagate to deeper layers of the ocean and can be associated (and not associated) with a change in the regime of the upper layers [29]. In the underlying layers, linear relationships with a zero time lag appear only in the southwestern region with $K_2\Delta H_{500}$, *NPGO*, *PDO* and *AD* indices. The estimates of the determination coefficient values (proportion of the explained variance is *D*, %) of the multiple regression of the fluctuation set of various climatic variables (CI) for the warm and cold (in parentheses) seasons and the first two EOF modes of the average annual anomalies of the integral heat content in the 5–200 m layer are given below:

$K_1\Delta Q_T$: $K_2\Delta H_{500}$, *NPGO*, *PDO*, *AD*: *D* = 89%,
($K_1\Delta Q_T$): $K_2\Delta H_{500}$, *NPGO*, *PDO*, *SOI*: *D* = 87%,
$K_2\Delta Q_T$: $K_1\Delta H_{500}$, *NPGO*: *D* = 37%,
($K_2\Delta Q_T$): *(*$K_1\Delta H_{500}$), *NP*, *H-NP*: *D* = 26%.

The estimates given above show that really statistically significant relationships between heat content variability and variations in the main climatic variables weaken with increasing mode number. In the study area, the processes parametrized by the *PDO* and *NPGO* indices in both seasons of the year make the greatest contribution to the first mode variability, and the *NPGO* index in the warm season – to the second mode variability (Table 3). In extratropical zones, changes in surface heat fluxes and ocean dynamics make the main contribution to the variations in the heat content of subsurface layers, and the processes associated with them cover a wide range of scales [30, 31]. The causes and mechanisms of the identified relationships are complex and ambiguous, and the main ones for the entire region of the subarctic Pacific Ocean were considered earlier [18, 20, 24, 32, 33]. Therefore, in order to avoid repetition, in this paper the emphasis is maid mainly on the assessment of their statistical significance over the past two decades.

Taking into account the revealed relationships, the main features of the interannual variability of the thermal condition characteristics of the region with large-scale processes in the ocean and atmosphere can be described (approximated) using a multiple regression equation of the dependent variable (*y*) and a group of independent variables. For example, in Fig. 7 the results of approximation, where the series of interannual fluctuations in the time coefficients of the first EOF mode ΔQ_T in the 5–200 m layer and SSTA for the NE region are selected as dependent variables, and the indices $K_2\Delta H_{500}$, *NPGO*, *PDO*, *SOI* (for the first variable) and *NPGO*, *PDO* (for the second one), are given as independent predictors. The correlation coefficient between these dependent variables characterizing the trends in changes in thermal conditions during 2000–2021 period is high – 0.93, and between the functions approximating them – 0.98.

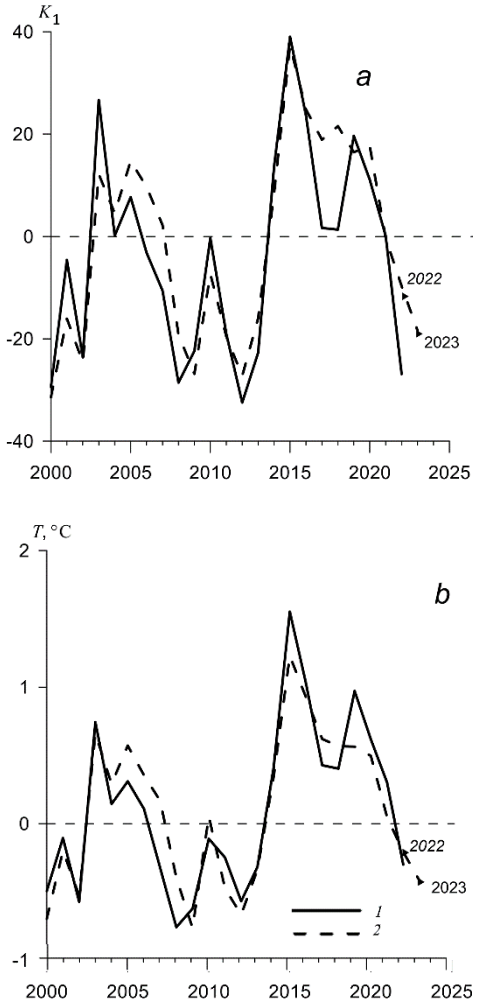

F i g. 7. Interannual changes in time coefficients of the EOF K_1 first mode ΔQT in the 5–200 m layer during the cold period of a year and the approximating values of the multiple regression equation (*a*); the same is for SST anomalies in the NE region (*b*). The years 2022 and 2023 on curves *2* denote the forecast estimates. Designations: *1* – the studied parameters, *2* – the approximating curves

Approximating curves *y* in Fig. 7 reproduce well the interannual changes in the dependent variables, including the extremely warm years of 2014–2016 and 2019–2020 [15]. By substituting the 5th-degree polynomial trend coefficients of these independent variables (climatic indices) into the multiple regression equation, we determined the trends of possible changes in thermal conditions in the next 2022, as well as taking into account the receipt of new data for the winter of 2021–2022, – in 2023. They indicate that the process of SSTA decrease (synchronously with the value of temporal coefficients of EOF ΔQ_T) after the maximum of 2019–2020 noted above may continue (Fig. 7), despite general growth trends for the entire region (see Table 1). At the same time, these "forecast estimates" for the coefficients of the first EOF mode ΔQ_T turned out to be somewhat worse than for SST, due to the insufficiently complete consideration of the possible list of predictors.

Conclusion

In the last two decades, the study area has been characterized by higher warming rates than during the same previous period, while the opposite trend was observed in the adjacent area of the northwestern Pacific Ocean. During the first decades of the 21st century, on average, for the entire water area of the northeastern part of the extratropical zone of the Pacific Ocean, the value of positive SST trends increased fourfold. In some years of this period, the largest positive anomalies of average annual SST values were formed in the northeastern and central regions of the water area, averaging ~ 1.3 ºC for the region.

Statistically significant trends in temperature and integral water temperature in separate layers of different sign and magnitude can be traced within the entire 1000-meter water column. The greatest positive trends in these characteristics are expressed in the upper 200–300 m layer in the northeastern and central regions of the water area as well. In general, over the past 20 years the heat content of the upper 200-meter layer has increased by 5%, and the 1000-meter layer – by 2%, which is 1.5 times less than in the northwestern sector of the Pacific Ocean extratropical zone, where, unlike the surface warming, the water column warming proceeded at a higher rate. One of the possible causes for the difference in the warming rate in these regions during the considered phases of climatic changes is the restructuring of the atmospheric circulation and, above all, changes in the position and severity of the Aleutian Low.

In the last two decades, the correlations of the integral temperature variations of the ocean upper layer with large-scale and regional processes in the ocean and atmosphere are manifested most extensively (in terms of the effect area, duration, and value of the correlation coefficient) through the following climatic indices: $K_{1\text{-}2}\Delta H_{500}$, *NPGO*, *PDO*, *NP*, *PNA*, *SOI*, *AD*, as well as *H-NP*. The density of statistically significant correlations weakens as the depth, the number of the leading oscillation mode and its contribution to the total variance of the integral temperature variability increase.

REFERENCES

1. Belkin, I., Krishfield, R. and Honjo, S., 2002. Decadal Variability of the North Pacific Polar Front: Subsurface Warming Versus Surface Cooling. *Geophysical Research Letters*, 29(9), pp. 65-1–65-4. doi:10.1029/2001GL013806

2. Saito, H., Suga, T., Hanawa, K. and Shikama, N., 2011. The Transition Region Mode Water of the North Pacific and Its Rapid Modification. *Journal of Physical Oceanography*, 41(9), pp. 1639-1658. doi:10.1175/2011JPO4346.1

3. Favorite, F., Dodimead, A.J. and Nasu, R., 1976. *Oceanography of the Subarctic Pacific Region, 1960-71*. International North Pacific Fisheries Commission Bulletin No. 33. Tokyo, Japan: Kenkyusha Printing Company, 187 p. Available at: https://waves-vagues.dfo-mpo.gc.ca/library-bibliotheque/17465.pdf [Accessed: 20 October 2022].

4. Qiu, B., 2002. Large-Scale Variability in the Midlatitude Subtropical and Subpolar North Pacific Ocean: Observations and Causes. *Journal of Physical Oceanography*, 32(1), pp. 353-375. doi:10.1175/1520-0485(2002)032<0353:LSVITM>2.0.CO;2

5. Kuroda, H., Suyama, S., Miyamoto, H., Setou, T. and Nakanowatari, T., 2021. Interdecadal Variability of the Western Subarctic Gyre in the North Pacific Ocean. *Deep Sea Research Part I: Oceanographic Research Papers*, 169, 103461. doi:10.1016/j.dsr.2020.103461

6. Barnett, T.P., 1981. On the Nature and Causes of Large-Scale Thermal Variability in the Central North Pacific Ocean. *Journal of Physical Oceanography*, 11(7), pp. 887-904. doi:10.1175/1520-0485(1981)011<0887:OTNACO>2.0.CO;2

7. Kwon, E.Y., Deutsch, C., Xie, S.-P., Schmidtko, S. and Cho, Y.-K., 2016. The North Pacific Oxygen Uptake Rates over the Past Half Century. *Journal of Climate*, 29(1), pp. 61-76. doi:10.1175/JCLI-D-14-00157.1

8. Rostov, I.D., Dmitrieva, E.V. and Rudykh, N.I., 2021. Climatic Changes of Thermal Conditions in the Pacific Subarctic at the Modern Stage of Global Warming. *Physical Oceanography*, 28(2), pp. 149-164. doi:10.22449/1573-160X-2021-2-149-164

9. Archer, C.L. and Caldeira, K., 2008. Historical Trends in the Jet Streams. *Geophysical Research Letters*, 35(8), L08803. doi:10.1029/2008GL033614

10. Nieves, V., Willis, J.K. and Patzert, W.C., 2015. Recent Hiatus Caused by Decadal Shift in Indo-Pacific Heating. *Science*, 349(6247), pp. 532-535. doi:10.1126/science.aaa4521

11. Trenberth, K.E. and Fasullo, J.T., 2013. An Apparent Hiatus in Global Warming? *Earth's Future*, 1(1), pp. 19-32. doi:10.1002/2013EF000165

12. Amaya, D.J., Miller, A.J., Xie, S.-P. and Kosaka, Y., 2020. Physical Drivers of the Summer 2019 North Pacific Marine Heatwave. *Nature Communications*, 11(1), 1903. doi:10.1038/s41467-020-15820-w

13. Bond, N.A., Cronin, M.F., Freeland, H. and Mantua, N., 2015. Causes and Impacts of the 2014 Warm Anomaly in the NE Pacific. *Geophysical Research Letters*, 42(9), pp. 3414-3420. doi:10.1002/2015GL063306

14. Loeb, N.G., Thorsen, T.J., Norris, J.R., Wang, H. and Su, W., 2018. Changes in Earth's Energy Budget during and after the "Pause" in Global Warming: An Observational Perspective. *Climate*, 6(3), 62. doi:10.3390/cli6030062

15. Ross, T., Jackson, J. and Hannah, C., 2021. The Northeast Pacific: Update on Marine Heatwave Status and Trends. *PICES Press*, 29(1), pp. 46-48. Available at: https://meetings.pices.int/publications/pices-press/volume29/PPJan2021.pdf#page=46 [Accessed: 20 October 2022].

16. Di Lorenzo, E. and Mantua, N., 2016. Multi-Year Persistence of the 2014/15 North Pacific Marine Heatwave. *Nature Climate Change*, 6(11), pp. 1042-1047. doi:10.1038/nclimate3082

17. Zhao, Y., Newman, M., Capotondi, A., Di Lorenzo, E. and Sun, D., 2021. Removing the Effects of Tropical Dynamics from North Pacific Climate Variability. *Journal of Climate*, 34(23), pp. 9249-9265. doi:10.1175/JCLI-D-21-0344.1

18. Rostov, I.D. and Dmitrieva, E.V., 2021. Regional Features of International Variations in Water Temperature in the Subarctic Pacific. *Russian Meteorology and Hydrology*, 46(2), pp. 106-114. doi:10.3103/S1068373921020059

19. Meehl, G.A., Hu, A., Arblaster, M., Fasullo, J. and Trenberth, K.E., 2013. Externally Forced and Internally Generated Decadal Climate Variability Associated with the Interdecadal Pacific Oscillation. *Journal of Climate*, 26(18), pp. 7298-7310. doi:10.1175/JCLI-D-12-00548.1

20. Hartmann, B. and Wendler, G., 2005. The Significance of the 1976 Pacific Climate Shift in the Climatology of Alaska. *Journal of Climate*, 18(22), pp. 4824-4839. doi:10.1175/JCLI3532.1

21. Na, H., Kim, K.-Y., Minobe, S. and Sasaki, Y.N., 2018. Interannual to Decadal Variability of the Upper-Ocean Heat Content in the Western North Pacific and Its Relationship to Oceanic and Atmospheric Variability. *Journal of Climate*, 31(13), pp. 5107-5125. doi:10.1175/JCLI-D-17-0506.1

22. Penny, S.G., Behringer, D.W., Carton, J.A. and Kalnay, E., 2015. A Hybrid Global Ocean Data Assimilation System at NCEP. *Monthly Weather Review*, 143(11), pp. 4660-4677. doi:10.1175/MWR-D-14-00376.1

23. Boyer, T.B., Baranova, O.K., Coleman, C., Garcia, H.E., Grodsky, A., Locarnini, R.A., Mishonov, A.V., Paver, C.R., Reagan, J.R. [et al.], 2018. *World Ocean Database 2018*. NOAA Atlas NESDIS 87. Silver Spring, MD: U.S. Department of Commerce, 207 p. Available at: https://www.ncei.noaa.gov/sites/default/files/2020-04/wod_intro_0.pdf [Accessed: 20 October 2022].

24. Rostov, I.D., Dmitrieva, E.V. and Rudykh, N.I., 2023. Interannual Variability of Thermal Characteristics of the Upper 1000-meter Layer in the Extratropical Zone of the Northwestern Part of the Pacific Ocean at the Turn of the XX-XXI Centuries. *Physical Oceanography*, 30(2), pp. 141-159. doi:10.29039/1573-160X-2023-2-141-159

25. Luchin, V.A. and Matveev, V.I., 2016. Interannual Variability of Thermal State of the Cold Subsurface Layer in the Okhotsk Sea. *Izvestiya TINRO*, 187(4), pp. 205-216. doi:10.26428/1606-9919-2016-187-205-216 (in Russian).

26. Gan, B., Wu, L., Jia, F., Li, S., Cai, W., Nakamura, H., Alexander, M.A. and Miller, A.J., 2017. On the Response of the Aleutian Low to Greenhouse Warming. *Journal of Climate*, 30(10), pp. 3907-3925. doi:10.1175/JCLI-D-15-0789.1

27. Xiu, P., Chai, F., Curchitser, E.N. and Castruccio, F.S., 2018. Future Changes in Coastal Upwelling Ecosystems with Global Warming: The Case of the California Current System. *Scientific Reports*, 8, 2866. doi:10.1038/s41598-018-21247-7

28. Overland, J.E., Adams, J.M. and Bond, N.A., 1999. Decadal Variability of the Aleutian Low and Its Relation to High-Latitude Circulation. *Journal of Climate*, 12(5), pp. 1542-1548. doi:10.1175/1520-0442(1999)012<1542:DVOTAL>2.0.CO;2

29. Stephens, C., Levitus, S., Antonov, J. and Boyer, T.P., 2001. On the Pacific Ocean Regime Shift. *Geophysical Research Letters*, 28(19), pp. 3721-3724. doi:10.1029/2000GL012813

30. Hu, Z., Hu, A. and Rosenbloom, N., 2020. Budgets for Decadal Variability in Pacific Ocean Heat Content. *Journal of Climate*, 33(17), pp. 7663-7678. doi:10.1175/JCLI-D-19-0360.1

31. Kelly, K.A., Small, R.J., Samelson, R.M., Qui, B., Joyce, T.M., Kwon, Y.-O. and Cronin, M.F., 2010. Western Boundary Currents and Frontal Air–Sea Interaction: Gulf Stream and Kuroshio Extension. *Journal of Climate*, 23(21), pp. 5644-5667. doi:10.1175/2010JCLI3346.1

32. Ceballos, L.I., Di Lorenzo, E., Hoyos, C.D., Schneider, N. and Taguchi, B., 2009. North Pacific Gyre Oscillation Synchronizes Climate Fluctuations in the Eastern and Western Boundary Systems. *Journal of Climate*, 22(19), pp. 5163-5174. doi:10.1175/2009JCLI2848.1

33. Deser, C., Phillips, A.S. and Hurrell, J.W., 2004. Pacific Interdecadal Climate Variability: Linkages between the Tropics and the North Pacific during Boreal Winter since 1900. *Journal of Climate*, 17(16), pp. 3109-3124. doi:10.1175/1520-0442(2004)017<3109:PICVLB>2.0.CO;2

About the authors:

Igor D. Rostov, Head of the Laboratory of Informatics and Ocean Monitoring, V.I. Il'ichev Pacific Oceanological Institute, Far Eastern Branch of Russian Academy of Sciences (43 Baltiyskaya Str., Vladivostok, 690041, Russian Federation), Ph.D. (Geogr.), **ORCID ID: 0000-0001-5081-7279**, rostov@poi.dvo.ru

Elena V. Dmitrieva, Senior Research Associate, V.I. Il'ichev Pacific Oceanological Institute, Far Eastern Branch of Russian Academy of Sciences (43 Baltiyskaya Str., Vladivostok, 690041, Russian Federation), Ph.D. (Tech.), **ORCID ID: 0000-0002-0094-5296**, e_dmitrieva@poi.dvo.ru

Natalia I. Rudykh, Senior Research Associate, V.I. Il'ichev Pacific Oceanological Institute, Far Eastern Branch of Russian Academy of Sciences (43 Baltiyskaya Str., Vladivostok, 690041, Russian Federation), Ph.D. (Geogr.), **ResearcherID: N-5821-2018**, rudykh@poi.dvo.ru

Contribution of the co-authors:

Igor D. Rostov – development of the article structure, processing and analysis of the data, writing the article text

Elena V. Dmitrieva – collection and processing of oceanographic data, calculations, drawing design, text editing

Natalia I. Rudykh – collection and processing of oceanographic data

The authors have read and approved the final manuscript.
The authors declare that they have no conflict of interest.